

# FLOW CHARACTERISTICS AND FORCES ACTING ON PIERS WITH DIFFERENT GEOMETRIES IN RIVES AT MEDIUM AND HIGH REYNOLDS` NUMBER

Nader Barahmand\*, Hamed Banavi

Department of Civil Engineering, Larestan Branch, Islamic Azad University, Larestan, IRAN

## ABSTRACT

Each year, many bridges are destroyed in the world, due to neglecting the role of hydraulic factors in design. Three important hydraulic reasons in bridge fracture are: unsuitable opening of aquifer, scour and immersing materials in water. Based on the studies carried out about bridge destruction, the flood flow making scour is known to be the main cause of bridge destruction. As the flood under the foundation or removes the bridge fabric. Due to the interaction of river with bridge structure, the role of hydraulic factors can not be neglected, therefore, it's necessary to estimate the maximum depth of scour around the piers to design the bridges piers economically and reliably. At present, the scientific principles of structural design of bridge pier has been well known. In contrast, there is not found any unique theory to estimate scour depth and the resultant force on bridge pier at high confidence. In this research, the effect of using vault and its diameter on the reduction of the forces acting on column and using rectangular and cylindrical columns at various speeds have been studied. This paper aims to investigate the water flow passing the bridge pier at various speeds. The three cylindrical, square and round-top wedge columns are used with flows passing at different speeds, the axial force on them are investigated. The contour of velocity, pressure and 3-D eddy behind the columns are taken into consideration. The range of Re is 10000 to 50000. The drag coefficient in all columns showed a decreasing trend versus Re. the drag of elliptical column had the lowest value. The greatest drag is related to square and column, the cylinder drag at high Re has a lower values than square and column which is due to pressure drag reduction from the movement of separation point to downstream resulting in smaller eddy behind the column and drag reduction.

Published on: 25<sup>th</sup>– Sept-2016

### KEY WORDS

bridge pier, square column, drag, cylindrical column

\*Corresponding author: Email: [nader\\_barahmand@yahoo.com](mailto:nader_barahmand@yahoo.com); Tel: +98-9177052312, +98-711-6254541, Fax: +98-711-6260909

## INTRODUCTION

Scour is a natural phenomenon happening from bed erosion and alluvial river side by water flow. Scour results in bridge fracture in flood flows. The presence of unstable flows and complexity of geometrical shapes of flow as the main reason of bridge fracture at flood, although immersed objects such as tress in the river flow can damage the bridge pier. One of the most important issues in the flow analysis and scour around bridge pier is flow separation influencing the drag force and fluctuates on bridge pier. The sharp and velocity of bridge pier have great effect on the size and power of eddies behind the column.

The research carried out on the forces on bridge pier and scour is taken to have long history. Inglis pona did numerous studies at water and electricity research center of india in 1938 and 1939 to study scour around bridge pier. This research was done in a flume with the sand of mean diameter 0.29 mm and became the basis of the relationship inglis pona.

Lee et al. (1961) studied the pier shape effect on scour depth. The rectangular pier makes the greatest scour depth. Making pier shape parallel with flow lines to reduce separation plays an important role in scour depth reduction in that in parallel cases, the power of horseshoe power decreases remarkable and less scour happens. If pier front is aerodynamic, the eddy power decreases.

Jane and Fischer (1979) the upstream landing number of bridge pier is important in scour. Therefore, in flows containing deposit, the scour around circular piers first decreases and then increases with the increase of landing number.

Melvile and Suferland (1988) determined that maximum depth of scour at cylindrical piers to be 2.46. This maximum depth decreases with the multiplication of factors while the scour is due to depositless water. Numerical

research by T-nishino et al. in 2007 on instability behind flow behind cylinder used combination of averaging methods and the method. [1]

### MATERIALS AND METHODS

Computational conditions and methods: The basis of computation is on finite blum element method. The turbulent viscose and instable flow is expressed in navier-stokes 3-D equal to m.

$$\frac{\partial}{\partial t} \int_{\Omega} \rho \vec{v} d\Omega + \int_{\Gamma} (\rho \vec{v} \cdot \hat{n}) d\Gamma = \int_{\Gamma} -P \hat{n} d\Gamma + \int_{\Gamma} \vec{\tau} \cdot \hat{n} d\Gamma + \int_{\Omega} \rho \vec{F}_b d\Omega \quad (1)$$

$$\frac{\partial \rho}{\partial t} + \vec{\nabla} \cdot \rho \vec{v} = 0 \quad (2)$$

In these equations, V is velocity and P is pressure, is tension tensor equal Newtonian fluid as and is volume force for mass unit. The numerical method is based on RI and Choi method and SIMPLE algorithm is used in velocity and presser couple.

The SIMPLE method used in this project is a prediction and modification method in that a guess is determined for velocity and pressure fields. As this guess is not necessarily true, it may not satisfy the continuity equation. After the following equations are extracted, pressure and velocity fields are so modified that the mass continuity is reinforced and finally the continuity equation is satisfied. Therefore, the modified fields of velocity and pressure satisfy momentum equation and continuity equation. The discrete equations of Navier and Stoke are expressed as the following:

$$\begin{aligned} a_p u_p^* + \sum_{n=nb} a_n u_n^* &= S_x - \Delta\Omega \frac{\partial P}{\partial x} \\ a_p v_p^* + \sum_{n=nb} a_n v_n^* &= S_y - \Delta\Omega \frac{\partial P}{\partial y} \\ a_p w_p^* + \sum_{n=nb} a_n w_n^* &= S_z - \Delta\Omega \frac{\partial P}{\partial z} \end{aligned} \quad (3)$$

Where is the multiplication of momentum source power on volume unit in i direction in cell volume and a coefficients are calculated for central subtraction interpolation.[2] The discreted equation of x direction for two adjacent cells P and E in RI and choo is as follows:

$$u_p + \left(\frac{\Delta\Omega}{a_p}\right)_p \left(\frac{\partial P}{\partial x}\right)_p = \left(\frac{S_x}{a_p}\right)_p - \left(\frac{1}{a_p} \sum_{n=nb} a_n u_n\right)_p \quad (4)$$

$$u_E + \left(\frac{\Delta\Omega}{a_p}\right)_E \left(\frac{\partial P}{\partial x}\right)_E = \left(\frac{S_x}{a_p}\right)_E - \left(\frac{1}{a_p} \sum_{n=nb} a_n u_n\right)_E \quad (5)$$

In this research, instable three dimensional time equations of basic pressure and the turbulence model is standard.

$$\mu_t = C_\mu \rho \frac{k^2}{\varepsilon} \quad (6)$$

The volume of , k & ε are obtained from semi-empirical equation, in which.

$$\rho \frac{\partial k}{\partial t} + \rho u_j k_{,j} = \left( \mu + \frac{\mu_t}{\sigma_k} k_{,j} \right)_{,j} + G + B - \rho \varepsilon \quad (7)$$

$$\rho \frac{\partial k}{\partial t} + \rho u_j k_{,j} = \left( \mu + \frac{\mu_t}{\sigma_k} k_{,j} \right)_{,j} + G + B - \rho \varepsilon \quad (8)$$

That at that ,  $C_1$ ,  $C_2$  and  $C_3$  are empirical coefficients  $\sigma_k$  and  $\sigma_\varepsilon$  are turbulent prantdl and Schmidt numbers, respectively. The terms  $c_1 \left( \frac{\varepsilon}{k} \right) G$  and  $c_2 \left( \frac{\varepsilon^2}{k} \right) G$  represent shear production  $\varepsilon$  and viscose  $\varepsilon$  delay .

The term  $c_1(1-C_3) \frac{\varepsilon}{k} B$  shows buoyancy effects. The term G represents turbulence kinetic energy from interaction between medium flow and turbulent flow field. The term B shows the buoyancy loss from density field of fluctuating field. [3]

Re number is defined as the following:

$$Re = \frac{\rho v C}{\mu} \quad (9)$$

in this formula,  $v$  is free flow velocity,  $\rho$  is free flow density, C is the reference level of body and  $\mu$  is kinetic viscosity.

$C_D$  is the drag coefficient .

$$C_D = \frac{D}{2U_\infty^2 S} \quad (9)$$

in which S is the surface covered by flow. [ Figure -1] boundary conditions and computational grid .The coordinates system is Cartesian (x,y,z).To solve the flow equations in the field around a round-tip wedged pier, we need a computational grid which divides flow field into small computational units. Solving the flow equations in all the computational units simultaneously results in the solution of the whole field. The grid around the interested geometry is a computational grid of hedragon structure chosen as c-type . In a profile of the solution grid is shown for structured grid around wedged column. As seen in the figure, the computation grid of hedradonal structure increases the accuracy in solving flow field and boundary layer estimation. It also helps to have better control on grid. [4]

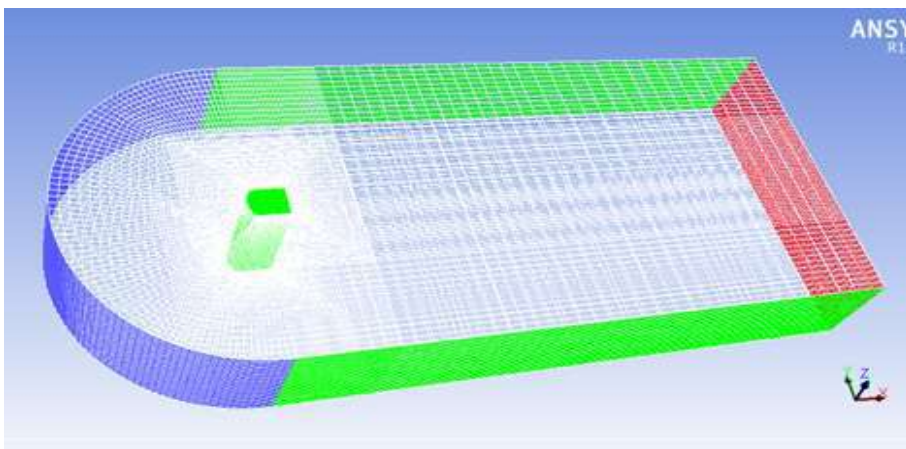


Fig: 1. 3-d grid view around wedged column

The independence of results from calculation grid are shown in Reynolds` number 60000 and the wedged column was obtained at range. in which d is the cylinder  $G_r$  diameter. For independency of results from time step, two steps of taken.

## RESULTS

### The results of solving flow around round-tip cylindrical column in fluid in different velocities

The contour of velocity, pressure, flow lines and eddy structure of flow at different Reynolds` number of 10000 are shown at [Figure- 2].As seen, the maximum of velocity is at corner arc of flow in column.

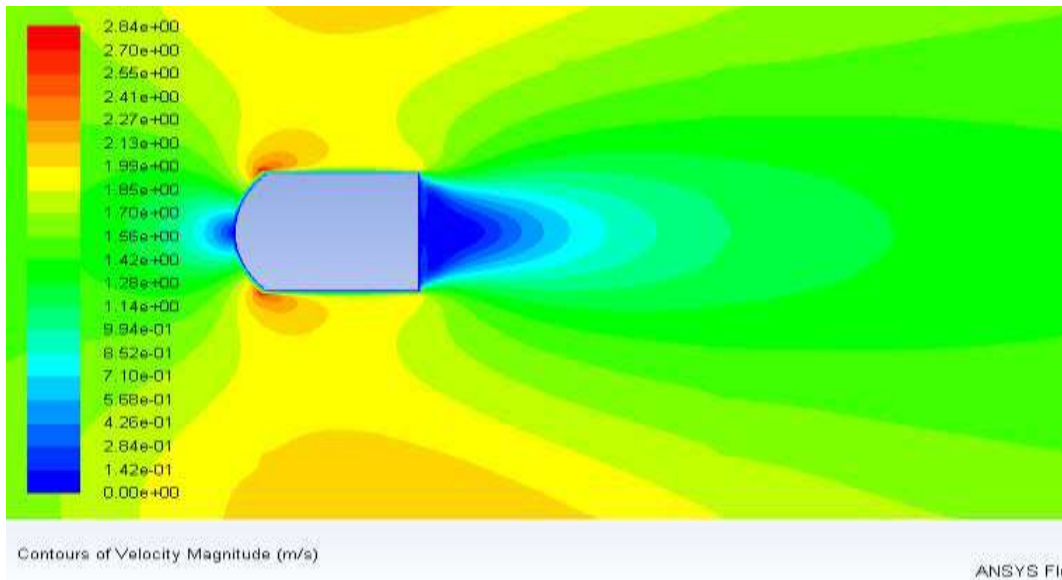


Fig: 2. velocity contour around wedged column at re=10000

The results of solving flow around cylindrical column in fluid in different velocities .As seen, the maximum of velocity is at the equinox of column. As seen in the figure, with the grid or organization , the border layer mash can be used more reliably, as in fig3 showing the organized mesh on border layer of pier making optimization and cell modification better than disorganized mesh , in turn increasing accuracy and reducing the error. As corner opposite the flow has lower velocity gradient , the flow does not separate from the corners while attached to the surface without any eddy. The maximum and minimum of velocity are increased and cover a larger area the same as eddy behind the object. [5 , 6]

The greatest pressure is on stagnation point and its maximum pressure and area increases. Increasing Reynolds` number increases the extent of eddy area the results of solving flow around square` column in fluid in different velocities. [7, 8 , 9]

The mesh grid around cylindrical pier` is seen in. As flow separation is important and there are formed specific trails behind the cylindrical piers , selection of grid and the number of points play important role in solving flow.

It is necessary to use organized mesh in border layer on pier to control increase or decrease the number of points on sphere surface and pier border layer so that separation site and forces are located carefully. shows the view of cylindrical pier on x-y direction. The symmetric conditions are in the top and bottom of the pier and wall conditions faraway and boundary conditions of velocity input and field exit were considered.

The volume of computational grid was about one million. In, the solution convergence and error are shown. [10 , 11]

## DISCUSSION

The contour of velocity , pressure, flow lines and eddy structure of flow at different Reynolds`

number of 50000 are shown at [Figure- 3]. the results of solving flow around square column in fluid in different velocities. the flow around square pier is symmetric and the maximum velocity occurs at sharp corner opposite the flow. Increasing Reynolds` number increases the velocity and enlarges the trails behind the column.



Fig: 3. Eddy around square column at  $re=50000$

The results of solving flow around round-tip cylindrical column in fluid in different angles .the contour of velocity, pressure, flow lines and eddy structure of flow at different Reynolds` number of 50000 are shown.

**As seen, the maximum of velocity is at corner arc of flow in column. AS seen, increasing Reynolds`**

number increases the maximal velocity covering a larger area and due to flow velocity and flow asymmetry , the area of maximal velocity is different on both sides of cylinder. Also, maximum pressure is seen to be in front of column. Increasing the flow velocity increases the area of maximal pressure. As seen from the pictures of flow lines around the object , increasing the Reynolds` number makes the left eddy larger than the right one due to the physical shape of the elliptical cylinder , causing inequality of force coefficient in x and y directions .At attack angle of zero degree , increasing Reynolds` number increases velocity and pressure reaching maximum at Reynolds` number of 60000. The greatest pressure forms at the side opposite the stagnation point and maximum pressure covers a great area. The increase of velocity increases the value and extent of this area. The pressure in eddy area is negligible. [12]

The results of solving flow around cylindrical column in fluid in different angles. As seen, the maximum of velocity is at the equinox of column. As seen, increasing Reynolds` number increases the maximal velocity covering a larger area. The stagnation point occurs at pole opposite the flow and flow separation happens behind the cylinder , reduced by increase of velocity [Figure-4]. the separation moves downstream with the increase of Reynolds` number of 6000 .

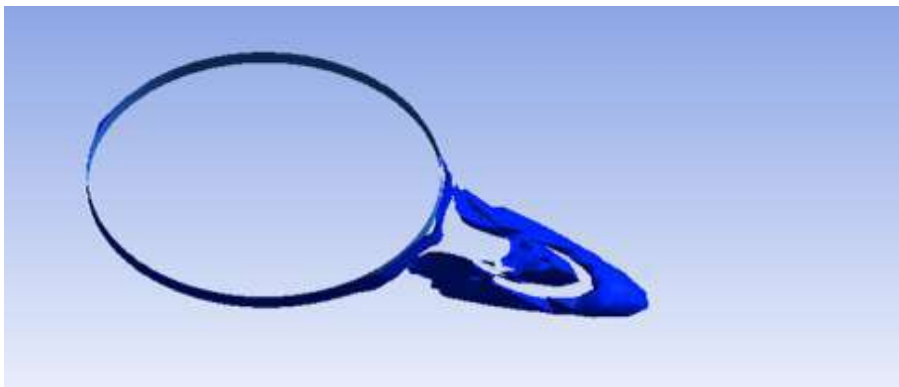


Fig: 4. Eddy around cylindrical column at  $re=60000$

### Comparison of drag change in columns

The changes of drag are seen in [Figure-5].

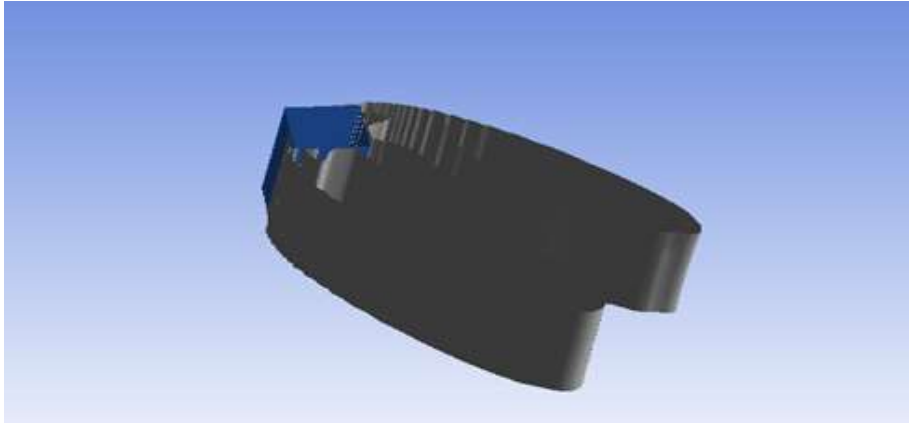


Fig: 5. Rotation area behind the column detected by rotation at  $re=70000$

### CONCLUSION

Fluid flow on the different shapes of column ,square, rectangle, sharp-tip wedged-like , parabola and elliptic at different Reynolds` number were investigated .The contour of velocity, pressure ,flow lines and eddy structure behind the columns are represented. In all columns, drag coefficient decreased with the increase of Reynolds` number. One of the important results of this project is stating that friction drag has little effect on total drag. For wedged column at 45 degrees, flow separation and flow non - recontact to surface have effect on reduction of drag coefficient.

### CONFLICT OF INTEREST

The author declares having no competing interests.

### ACKNOWLEDGEMENT

None

### FINANCIAL DISCLOSURE

None

### REFERENCES

- [1] Jain and Fischer. [1979]"scour around circular bridge piers at high froude number,pp.4-5
- [2] Jain SC, Fischer EE. [1979] Scour around circular bridge pier at high Froudemumber, Report FHWA- RD- 79-104, PP.308-317
- [3] Melville and Sutherland. [1988] Design method for local scour at bridge pier, *Journalof Hydraulic Engineering*, 114(10).
- [4] Thamer AM, Megat Johari M, Ghazali AH, Huat BK. [2005] Validation of somebridge pier scour formulae using field data and laboratoty data, *American Journal ofEnvironmental Science*,pp.119-125,
- [5] Ansari SA, Kothiyari UC, Ramga KG. [2002] Influence of cohesion on scour around Bridge piers, *Journal of Hydraulic Research*, 40(6): 717-729.
- [6] Baker CJ. [1980] Theoretical approach to prediction of local scour around bridge piers", *Journal of Hydraulic Research*,18(1).
- [7] Boehmler EM, Olimpio JR. [2000] Evaluation of pier – scour measurement me thods and pier scour prediction with observed



- scour measurement at selected bridge sites in new Hampshire, 1995-98, Water Resources Investigation, Report 00-4183.
- [8] Bozkus Z, Yildiz O. [2004] Effects of inclination of bridge piers on scouring depth, *Journal of Hydraulic Engineering*, 130(9):905-913.
- [9] Breusers HNC. [1977] Local scour around cylindrical piers, *Journal of Hydraulic Research*, 15:211-215.
- [10] Chang WY, Lai JS, Yen CL. [2004] Evolution of scour depth at circular bridge piers, *Journal of Hydraulic Engineering*, 130(9):905-913.
- [11] Chiew YM. [1992] Scour protection at bridge piers, *Journal of Hydraulic engineering*, 118(9)
- [12] Ettema R. [1980] Scour at bridge pier, Dept of civil Engineering university of auckland, New zealand, No. 216.